Estimation of statistical atlases using groups of diffeomorphisms

Monica Hernandez, Matias N. Bossa, and Salvador Olmos

Aragon Institute of Engineering Research (I3A)
University of Zaragoza, Spain

Abstract. This article addresses the issue of estimation of statistical atlases that describe the average and the variability of a population of anatomical images. Our work is based on Computational Anatomy where anatomical variability is characterized by the deformations existing between a reference image and each element of the population. This characterization allows to translate the study of the statistical variability from the set of anatomical images to the infinite dimensional Lie group of diffeomorphisms where the necessary mathematical setting for statistical analysis has been recently developed. Our contribution goes in two directions. First, we propose a novel algorithm for diffeomorphic registration where the optimization is performed on one-parameter subgroups of the group of diffeomorphisms. We show that this algorithm outperforms other previous approaches in terms of image matching, deformation smoothness and computational complexity. Second, we describe a framework for the estimation of the average and the principal geodesics in the infinite dimensional Lie group of diffeomorphisms applied to the generation of statistical atlases of brain images.

Key words: Statistical brain atlas, Computational Anatomy, Lie group, diffeomorphism, Principal Geodesic Analysis

1 Introduction

The estimation of brain atlases from anatomical images is of great relevance due to its multiple applications, as template-based segmentation, modeling of anatomical variability, and brain mapping, among others [1–3]. Atlases have been crucial to understand the variability of brain anatomy in longitudinal and transversal studies allowing hypothesis testing and improving the diagnosis of mental diseases such as schizophrenia or Alzheimer's disease [4, 5].

Most of the atlases are based on a single subject ([3] and references therein). Their application is limited to images close to the template and cannot be generalized to anatomies presenting large variability without introducing an important bias. To address with this bias, several authors propose to estimate a statistically representative average template for the population of images. The majority of the methods for average atlas estimation are based on Computational Anatomy, that proposes to parametrize anatomical variability by the deformations existing between the elements of the population of images. This parametrization allows to translate the study of the statistical variability from the sample of images to the associated deformations. Thus, the average atlas is computed from the estimated average transformation.

Some works compute the average transformation performing linear average of the displacement fields associated to the sample transformations [6, 7]. Although

these techniques provide acceptable results with transformations in the small deformation setting, the space of displacement fields is not a linear space and, therefore, linear averaging could give rise to non plausible results in anatomical images with high variability. As an alternative, the computation of the average transformation is usually approached with the theory of large deformations that results more appropriate when dealing with anatomical images [8–11].

Transformations in the large deformation setting are assumed to be in the infinite dimensional Lie group of diffeomorphisms. The mathematical framework for the computation of average and principal geodesics has been deeply studied for finite dimensional Lie groups [12, 13]. This framework can be extended to the infinite dimensional Lie group of diffeomorphisms once some of the elements of this Riemannian manifold are identified. Among others, these elements are the tangent space, the geodesics and the exponential and logarithm maps. All of them have been described in the theory of classical mechanics [14]. In the last years, Computational Anatomy has focused on the computation of the exponential and the logarithm maps towards the estimation of the average and principal geodesics in the group of diffeomorphisms [8, 9, 15, 10, 16]. To our knowledge, no proposal there exists for Principal Geodesic Analysis (PGA) in the group of diffeomorphisms.

Our work intends to embed the mathematical setting for statistical analysis on the infinite dimensional Lie group of diffeomorphisms into the large deformation theory to provide a framework for the estimation of statistical atlases from populations of anatomical images. Our contribution goes in two directions. First, we propose a novel method for diffeomorphic registration that outperforms other previous approaches in terms of image matching, deformation smoothness and computational complexity. Second, we extend the framework for the computation of the average and the modes of variation in [12, 13] to the infinite dimensional Lie group of diffeomorphisms with application to the estimation of statistical atlases in brain imaging.

The rest of the article is divided as follows. In Section 2 we present our method for the computation of diffeomorphisms. Section 3 focuses on the framework for the estimation of statistical atlases. The results are presented in Section 4. Finally, Section 5 presents discussion and some concluding remarks.

2 Diffeomorphic registration between anatomical images

Let Ω be a subset of points in $\mathbb{R}^n$. A diffeomorphism is a smooth continuous mapping $\varphi : \Omega \to \Omega$ with smooth and continuous inverse. The set of diffeomorphisms $Diff(\Omega)$ constitute an infinite dimensional Riemannian manifold where the tangent space at the identity V, is the space of vector fields in Ω.

In Computational Anatomy, images are considered as diffeomorphic deformations of a reference image plus additive noise, $I = I_{ref} \circ \varphi + n$. The noise term accounts for anatomical details that cannot be explained by φ as well as for photometric variations. A diffeomorphism connecting two images $I_0, I_1 : \Omega \to \mathbb{R}$ is represented by the end point $\varphi = \phi(1)$ of a path or flow of diffeomorphisms in the Riemannian manifold, $\phi(t) : [0, 1] \to Diff(\Omega)$. This path is usually computed from its corresponding flow of vector fields in the tangent space $v(t) : [0, 1] \to V$ by the transport equation $\dot{\phi}(t) = v(t, \phi(t))$ [14]. Thus, the optimal diffeomorphic path connecting I_0 to I_1 is computed from the minimization of the energy functional

$$E_{I_0 \to I_1}(v(t)) = \int_0^1 \|v(t)\|_V^2 dt + \frac{1}{\sigma^2} \|I_0 \circ \varphi^{-1} - I_1\|_{L^2}^2 \quad (1)$$

where v and ϕ satisfy the transport equation, $\|\cdot\|_V$ measures the amount of deformation of the associated diffeomorphism, $\|\cdot\|_{L^2}$ measures the similarity between the images, and σ is a scaling factor that balances the similarity of the images and the smoothness of the diffeomorphism. As a result, the solution the optimization of Equation 1 provides a geodesic path in $Diff(\Omega)$.

In contrast to Computational Anatomy, our framework considers $Diff(\Omega)$ not only as a Riemannian manifold but also as an infinite dimensional Lie group together with the composition of diffeomorphisms. As in the case of finite dimensional Lie groups, geodesics in $Diff(\Omega)$ are identified with one-parameter subgroups. Each $v \in V$ spans a unique one-parameter subgroup of diffeomorphisms $Diff_v(\Omega) = (\phi(s))_{s\in\mathbb{R}}$. The elements in $Diff_v(\Omega)$ are solution of the stationary transport equation $\dot{\phi}(t) = s \cdot v(\phi(t))$ with initial condition $\phi(0) = e$ and constitute geodesics in $Diff(\Omega)$ with infinitesimal generator $v = \frac{\partial}{\partial t}\phi(t) \mid_{t=0}$. These elements are of the form $\exp(sv)$, $s \in \mathbb{R}$, where $\exp : V \to Diff(\Omega)$ is the exponential map.

Thus, our method for the computation of diffeomorphisms between anatomical images assumes that φ belongs to a one-parameter subgroup $Diff_w(\Omega)$ for some infinitesimal generator $w \in V$. Thus, the diffeomorphism that connects I_0 and I_1 is represented by $\exp(w)$, where w is computed from the minimization of the energy functional $E_{I_0\to I_1}(w) = \|w\|_V^2 + \frac{1}{\sigma^2}\|I_0 \circ \exp(w)^{-1} - I_1\|_{L^2}^2$. In order to assure a source to target symmetry in the registration we use the inverse-consistent version instead

$$E_{I_0\leftrightarrow I_1}(w) = \|w\|_V^2 + \frac{1}{\sigma^2}\left(\|I_0 \circ \exp(w)^{-1} - I_1\|_{L^2}^2 + \|I_1 \circ \exp(w) - I_0\|_{L^2}^2\right) \quad (2)$$

The Euler-Lagrange equation associated to the minimization of the energy functional is $\nabla_w E_{I_0\leftrightarrow I_1}(w) = 2w - (LL^\dagger)^{-1}\left(\frac{2}{\sigma^2}(I_0 \circ \exp(w)^{-1} - I_1)\nabla(I_0 \circ \exp(w)^{-1})\right)$ $+(LL^\dagger)^{-1}\left(\frac{2}{\sigma^2}(I_1 \circ \exp(w) - I_0)\nabla(I_1 \circ \exp(w))\right)$, where L is a linear differential operator associated to the $\|\cdot\|_V$.

The numerical implementation for finding the minimum of the energy functional proceeds in a gradient descent fashion using a golden search strategy to update the step size ϵ. The algorithm initializes with iteration $k = 0$, $w = 0_V$, and $\varphi = e$. Every iteration in the gradient descent consists of the following steps: 1) Compute $\nabla_{w_k} E(w_k)$ from the Euler-Lagrange Equation. 2) Update the gradient descent step $w_k = w_{k-1} - \epsilon\nabla_{w_{k-1}} E(w_{k-1})$. 3) Compute the inverse diffeomorphimsm $\varphi^{-1} = \exp(-w_k)$. 4) Compute the direct diffeomorphism $\varphi = \exp(w_k)$. 5) Compute the transformed images $I_0 \circ \varphi^{-1}$ and $I_1 \circ \varphi$. 6) Check for convergence criterion. The computation of the exponential map is performed using the extension of the *Scaling and Squaring* method to diffeomorphisms [16]. The rest of the implementation details are similar to those found in [15].

3 Estimation of statistical atlases

In Computational Anatomy, the notion of similarity between images connected by diffeomorphic registration is defined from the metric in $Diff(\Omega)$. Two images are similar if the diffeomorphism with minimal norm existing between them provides a small amount of deformation [17, 10]. Given $I_1, ..., I_N$ a set of sample images the average atlas can be defined as the anatomical image that minimizes the amount of diffeomorphic deformation necessary to match with all the sample images simultaneously. This definition allows to translate the study of the anatomical variability from the sample of images to their associated diffeomorphisms. The

benefit is that statistical analysis can be performed extending the techniques previously developed for finite dimensional Lie groups to the infinite dimensional Lie group of diffeomorphisms. In order to compute the average and perform statistical analysis, we must assume that all the diffeomorphisms involved in the computations belong to one-parameter subgroups to guarantee the existence of the inverse of the exponential map (logarithm map). Thus, given I_{ref} initial estimate of the average atlas, and $\varphi_i \in Diff_{w_i}(\Omega)$ such that $I_i = I_{ref} \circ \varphi_i + n_i$, $i = 1, ..., N$, the computation of the average atlas $\bar{I}$ can be translated to the computation of the average diffeomorphism $\bar{\varphi}$ associated to the φ_i in the Lie group $Diff(\Omega)$ by means of $\bar{I} = I_{ref} \circ \bar{\varphi}$. An scheme of this framework is shown in Figure 1.

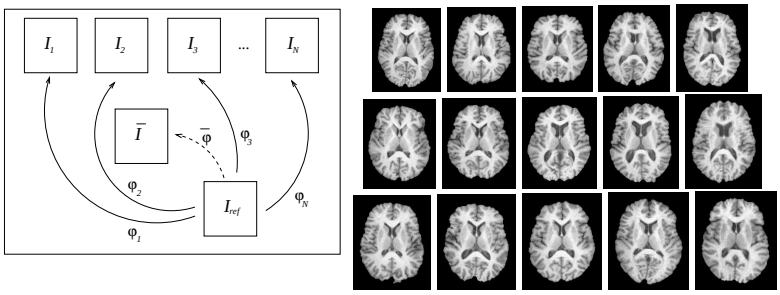

Fig. 1. Left, framework for the computation of the average atlas. Right, dataset of images used for atlas estimation in the experimental section.

The average diffeomorphism is defined as the intrinsic or Karcher average [13, 12] in the manifold $Diff(\Omega)$, $\bar{\varphi} = \arg\min_{\varphi} \sum_{i=1}^{N} \| \log(\varphi_i \circ \varphi^{-1}) \|_V^2$. The computation of the average diffeomorphism proceeds in a gradient descent on the manifold of diffeomorphisms

$$\bar{\varphi}_{(k+1)} = \exp\left(\frac{1}{N} \sum_{i=1}^{N} \log\left(\varphi_i \circ \bar{\varphi}_{(k)}^{-1} \right) \right) \circ \bar{\varphi}_{(k)} \tag{3}$$

The algorithm is initialized with iteration $k = 0$, $\bar{\varphi}_{(0)} = e$ and φ_i solution of the diffeomorphic registration $E_{I_i \leftrightarrow I_{ref}}(w_i)$. The exponential and logarithm maps are computed using the method proposed in [16]. The convergence in the gradient descent is reached when $\| \sum_{i=1}^{N} \log(\varphi_i \circ \varphi_{(k)}^{-1}) \|_V^2$ is under a tolerance value.

In order to reduce the bias introduced by the selection of I_{ref}, we propose to include the gradient descent for the computation of $\bar{\varphi}$ in an iterative algorithm that re-estimates I_{ref} and φ_i subsequently. The algorithm is initialized with I_{ref} equal to the element from the population of images that minimizes $\sum_{i \neq j} \|w_i\|_V^2 + (1/\sigma^2) \|I_i \circ \varphi_i^{-1} - I_j\|_{L^2}^2$. Then, $\bar{\varphi}$ is computed from the gradient descent on $Diff(\Omega)$ (Equation 3). At this point, the images $I_i \circ \varphi_i^{-1} \circ \bar{\varphi}$, that can be expressed as $I_{ref} \circ \bar{\varphi} + n_i \circ \varphi_i^{-1} \circ \bar{\varphi}$, constitute a cloud of points in a neighborhood of $I_{ref} \circ \bar{\varphi}$. In this neighborhood we can approximate the new I_{ref} by the linear average $\frac{1}{N} \sum_{i=1}^{N} (I_i \circ \varphi_i^{-1} \circ \bar{\varphi})$, thus reducing the noise variance. The diffeomorphic registration $E_{I_i \leftrightarrow I_{ref}}(w_i)$ allows to compute φ_i in the following iteration. The convergence is reached when $\|I_{ref}^{(k)} - I_{ref}^{(k-1)}\|_{L^2}^2$ is less than a tolerance value. The final estimated average atlas is I_{ref}.

At this point, any multivariate statistical technique can be used to analyze the variability from the average. For example, the computation of the modes of variation can be done with Principal Geodesic Analysis (PGA) on the residuals

w_i, solution to the variational problem $E_{I_i \leftrightarrow \bar{I}}(w_i)$. In terms of the canonical basis in V, the residuals can be written as $u_i = \text{vec}(w_i)$, where vec represents a matrix vectorization. Singular value decomposition (SVD) of the residual matrix $R = (u_1|...|u_N)$ provides the direction of the principal geodesics and the energy associated to each mode of variation $(u_{(k)}, s^2_{(k)})$. Analogously to PGA in the finite dimensional case, we can choose a subset of $n \leq N$ principal directions sufficient to describe a percentage of the variability of the population. New instances in the statistical atlas can be generated from $I = \bar{I} \circ \varphi$ where $\varphi = \exp\left(\sum_{i=1}^{n} \alpha_{(i)} u_{(i)}\right)$ and $\alpha_{(i)}$ are chosen within $[-3s_{(i)}, 3s_{(i)}]$.

4 Results

4.1 Datasets

In order to evaluate the performance of diffeomorphic registration and atlas estimation, a set of 15 T1-MRI images was used. The images were acquired using a General Electric Signa Horizon CV 1.5 Tesla scan. As preprocessing steps, the images were resampled yielding an spatial resolution of $0.9 \times 0.9 \times 0.9$ mm, the skull was removed from the images using [18], the image intensity was normalized using a histogram matching algorithm, and aligned to a common coordinate system using a similarity transformation (7 dof). We present the results in the 2D axial slices shown in Figure 1.

Table 1. Average and standard deviation of the relative L^2 differences, $RSSD$, and the extrema of the jacobian determinant, J_{max}, J_{min}. Left and right tables show the results obtained with $E_{I_0 \leftrightarrow I_1}(v(t))$ and $E_{I_0 \leftrightarrow I_1}(w)$, respectively.

$1/\sigma^2$	$RSSD$	J_{max}	J_{min}
1e4	0.57 ± 0.03	3.24 ± 0.50	-0.12 ± 0.06
2.5e4	0.41 ± 0.03	5.13 ± 1.00	-1.16 ± 0.48
5e4	0.33 ± 0.02	6.90 ± 1.29	-3.78 ± 2.10
7.5e4	0.29 ± 0.02	8.43 ± 2.25	-7.03 ± 4.45
1e5	0.27 ± 0.02	9.42 ± 2.92	-9.05 ± 5.30

$1/\sigma^2$	$RSSD$	J_{max}	J_{min}
1e4	0.56 ± 0.03	3.76 ± 0.64	0.23 ± 0.04
2.5e4	0.38 ± 0.03	6.54 ± 1.56	0.09 ± 0.03
5e4	0.27 ± 0.03	8.04 ± 1.66	0.04 ± 0.03
7.5e4	0.22 ± 0.03	9.59 ± 2.40	-0.03 ± 0.22
1e5	0.19 ± 0.03	10.65 ± 2.62	-0.13 ± 0.33

4.2 Diffeomorphic registration performance.

In this experiment, we compare the inverse consistent version of the diffeomorphic registration in [15] ($E_{I_0 \leftrightarrow I_1}(v(t))$) with our method ($E_{I_0 \leftrightarrow I_1}(w)$). The quality of the registration is measured with parameters based not only on the final image matching but also on the transformation smoothness. These performance parameters are strongly influenced by the selection of the scaling parameter σ. The experiment consists in the registration of one of the images in our dataset to the rest of images with several values for σ. The image matching is quantified from the relative L^2 differences, $RSSD = (1/2)(\|I_0 \circ \varphi^{-1} - I_1\|_{L^2} + \|I_1 \circ \varphi - I_0\|_{L^2})/\|I_0 - I_1\|_{L^2}$, and the smoothness of the transformation is measured from the extrema of the jacobian determinant associated to the inverse transformation, $J_{max} = \max(\det(D\varphi^{-1}))$ and $J_{min} = \min(\det(D\varphi^{-1}))$. Table 1 presents the average and standard deviation of these measurements. Registrations with better performance are those where the relative differences are low while the jacobian determinant remains greater than

zero. In the following, we select the parameter $1/\sigma^2$ equal to $5e4$, that guarantees the transformation invertibility with maximum matching for our algorithm. In Figures 2 and 3 we show a representative example of diffeomorphic registration with this parameter setting.

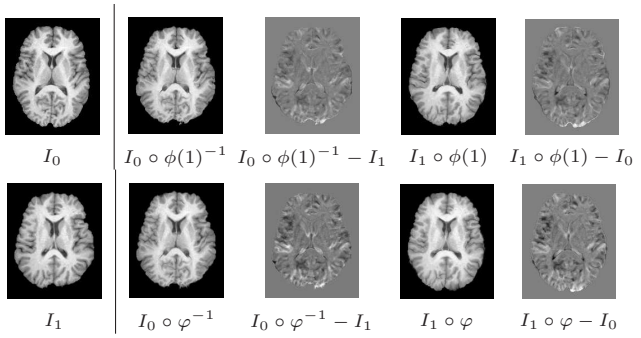

Fig. 2. Illustration of one of the registration experiments with $1/\sigma^2 = 5e4$. The first column shows the template and target images used for registration. The upper row shows the results obtained with $E_{I_0 \leftrightarrow I_1}(v(t))$. The lower row shows the results obtained with $E_{I_0 \leftrightarrow I_1}(w)$). To be comparable, the rank of the differences has been normalized to the same intervals.

4.3 Average atlas estimation.

In this experiment, we present the average and the modes of variation estimated with the method proposed in Section 3. Figure 4 shows the average atlas in contrast with the linear average of the sample images, and the images associated to the modes of variation.

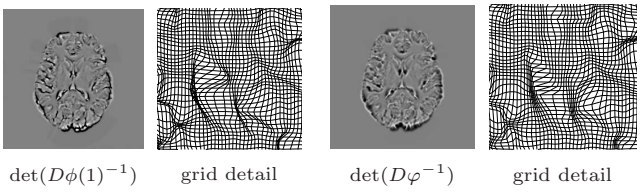

Fig. 3. Jacobian determinant (represented in logarithm scale) and grid details of one of the registration experiments. The two leftmost figures show the results obtained with $E_{I_0 \leftrightarrow I_1}(v(t))$. The two rightmost figures show the results obtained with $E_{I_0 \leftrightarrow I_1}(w)$).

5 Discussion and conclusions

In this article, we have presented a framework for diffeomorphic registration and statistical atlas estimation based on the Riemannian geometry of the infinite dimensional Lie group of diffeomorphisms. The method for diffeomorphic registration estimates the optimal transformation connecting two anatomical images in one-parameter subgroups of diffeomorphisms and, therefore, can be computed from the exponential map of its infinitesimal generator. In contrast, traditional methods for diffeomorphic registration consider that the transformations are made of composition of geodesics associated to time varying vector fields. The performance

of our algorithm has been compared with one of these methods [15] in a set of 15 axial MRI slices. Although both algorithms present similar accuracy (average $RSSD < 30\%$), all transformations obtained with the method using time varying vector fields are not invertible and, therefore, not diffeomorphic. Even though the set of diffeomorphisms associated to time varying vector fields includes the set diffeomorphisms associated to stationary vector fields, the performance in our dataset is better in the last case. Besides, our algorithm provides a considerable reduction of the computational requirements for diffeomorphic registration.

Our method for diffeomorphic registration has been included in a framework for the computation of the average and the modes of variation of a population of images. The framework generalizes existing techniques for statistical analysis in finite dimensional Lie groups to infinite dimension. Some other works have proposed methods for the computation of the average atlas based on diffeomorphic registration different from ours in the strategies for registration, selection of the reference image and the manifold in which the gradient descent is performed [8–10]. These algorithms usually assume that the diffeomorphisms are associated to time varying vector fields. From our experience, the registration constitutes a critical stage in the computation of the average and, therefore, our algorithm for diffeomorphic registration could improve the performance in these algorithms while introducing computational efficiency. In addition, the logarithm map is not well defined for diffeomorphisms associated to non stationary velocity fields. Therefore, these methods cannot guarantee the convergence to the population average defined as the minimization of the amount of deformation and the modes of variation cannot be computed in their framework.

In our work, the resulting average atlas is presented in comparison to the linear average image. As long as the anatomical details in the linear average are blurred, the details in the average atlas remain sharp while representing the average of the population of images. While the average atlas presents a left-right lateral symmetry the dominant modes of variation present both symmetric and asymmetric deformations visible at the lateral ventricles and the cortex. Finally, it is interesting to remark that the anatomical variability within the population of images is illustrated by the modes of variation and non-plausible images are absent in the first six modes of variation.

The experiments presented in this article were performed in 2D axial slices. Although the methodology is straightforwardly applicable to the 3D case, we found that the computation of the diffeomorphic registration and the logarithm map are unaffordable in a standard computer and a reasonable interval of time. We are currently working in a multiresolution strategy for registration and an algorithm for the computation of the logarithm map in order to reduce the computational requirements and provide results in 3D datasets.

References

1. Heckemann, R.A., Hajnal, J.V., Aljabar, P., Rueckert, D., Hammers, A.: Automatic anatomical brain MRI segmentation combining label propagation and decision fusion. Neuroimage **33(1)** (2006) 115 – 126
2. Xue, Z., Shen, D., Karacali, B., Stern, J., Rottenberg, D., Davatzikos, C.: Simulating deformations of MR brain images for validation of atlas-based segmentation and registration algorithm. Neuroimage **33(3)** (2006) 855 – 866
3. Thompson, P.M., Woods, R.P., Mega, M.S., Toga, A.W.: Mathematical/computational challenges in creating deformable and probabilistic atlases of the human brain. Hum. Brain Map. **9** (2000) 81 – 92

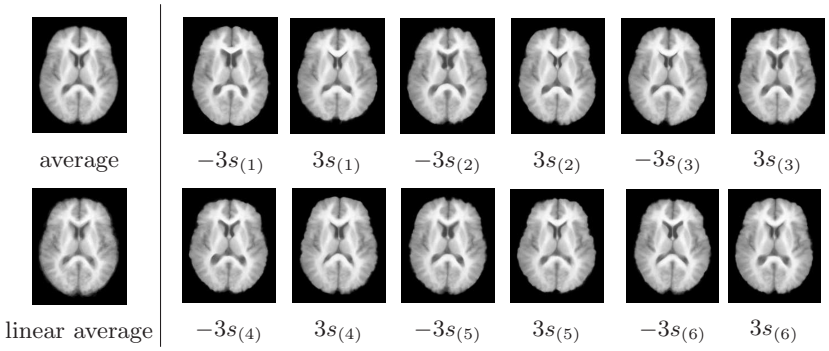

Fig. 4. Left, average atlases. The upper image shows the average atlas computed with our method. For comparison, the lower image shows the average atlas computed from linear averaging. Right, first six modes of variation of the statistical atlas. Each pair of images show the modes corresponding to $\{-3s_{(k)}, 3s_{(k)}\}$ along the k-th principal geodesic.

4. Yushkevich, P., Dubb, A., Xie, Z., Gur, R., Gee, J.: Regional structural characterization of the brain of schizophrenia patients. Acad. Radiol. **12(10)** (2005) 1250 – 1261
5. Carmichael, O.T., Aizenstein, H.A., Davis, S.W., Becker, J.T., Thompson, P.M., Meltzer, C.C., Liu, Y.: Atlas-based hippocampus segmentation in Alzheimer's disease and mild cognitive impairment. Neuroimage **27(4)** (2005) 979 – 990
6. Guimond, A., Meunier, J., Thirion, J.P.: Average brain models: A convergence study. Comput. Vis. Image Underst. **77(2)** (2000) 192 – 210
7. Bathia, K., Hajnal, J., Puri, B., Edwards, A., Rueckert, D.: Consistent group-wise non-rigid registration for atlas construction. IEEE International Symposium on Biomedical Imaging (ISBI 2004) (2004) 908 – 911
8. Joshi, S., Davis, B., Jomier, M., Gerig, G.: Unbiased diffeomorphic atlas construction for compuational anatomy. Neuroimage **23** (2004) 151 – 160
9. Avants, B., Gee, J.: Geodesic estimation for large deformation anatomical shape averaging and interpolation. Neuroimage **23** (2004) 139 – 150
10. Beg, M.F., Khan, A.: Computing an average anatomical atlas using LDMM and geodesic shooting. IEEE International Symposium on Biomedical Imaging (ISBI 2006) (2006) 1116 – 1119
11. Garcin, L., Younes, L.: Geodesic matching with free extremities. J. Math. Imaging Vis. **25** (2006) 329 – 340
12. Pennec, X.: Intrinsic statistics on Riemmanian manifolds: Basic tools for geometric measurements. J. Math. Imag. Vis. **25(1)** (2006) 127 – 154
13. Fletcher, P.T., Joshi, S., Lu, C., Pizer, S.M.: Principal geodesic analysis for the study of nonlinear statistics of shape. IEEE Trans. Med. Imaging **23(8)** (2004) 994 – 1005
14. Arnold, V.: Mathematical methods of classical mechanics. Springer-Verlag, Berlin, Germany (1989)
15. Beg, M.F., Miller, M.I., Trouve, A., Younes, L.: Computing large deformation metric mappings via geodesic flows of diffeomorphisms. Int. J. Comput. Vis. **61 (2)** (2005) 139–157
16. Arsigny, V., Commonwick, O., Pennec, X., Ayache, N.: Statistics on diffeomorphisms in a Log-Euclidean framework. MICCAI 2006, Lecture Notes in Computer Science (LNCS), Springer-Verlag, Berlin, Germany **4190** (2006) 924 – 931
17. Grenander, U., Miller, M.: Computational Anatomy: an emerging discipline. Quaterly of Applied Mathematics **56** (1998) 617 – 694
18. Dodgas, B., Sattuck, D.W., Leahy, R.M.: Segmentation of skull and scalp in 3D human MRI using mathematical morphology. Hum. Brain Map. (2005)